



10-1-14

APPLICATION OF AN ALTERNATE METHOD INCLUDING FOUNDATION EFFECT FOR ARCH DAM SEISMIC ANALYSIS

Li-Ming CHEN

Hydraulic Engineering Department, Sinotech Engineering Consultants, Inc.

SUMMARY

This paper introduces the use of the Strip Compliance Method to determine the stiffness and radiation damping of dam foundation, in a form suited to the SAPIV program, for economically and properly representing the foundation-structure interaction in arch dam seismic analysis. The stiffness and damping of foundation are obtained from compliance in four major directions for an infinite rigid massless strip resting on an elastic half space, which need to be transformed to be consistent with nodal degrees of freedom at the interface with the dam's finite-element model. The conventional Vogt's Constant Method is also presented for comparison.

INTRODUCTION

Normally, three dimensional finite element modeling of an arch dam in stress analysis requires that a significant portion of the dam foundation be included to properly represent the foundation-structure interaction. However, this is not only costly from a computer usage point of view due to the large number of degrees of freedom, but is impractical for seismic analysis. Therefore, an alternate method called the Strip Compliance Method is proposed to economically and reasonably simulate the foundation effects in seismic analysis.

In the Strip Compliance Method foundation effects are represented by three-component discrete impedance elements at the nodes of the dam's finite element model located at its interface with the foundation. The stiffness and damping of impedance elements can be estimated by obtaining the compliance function for an infinite rigid massless strip of a definite width resting on an elastic half space.

By using the SAPIV program, this method was applied to the time-history response analysis for the Feitsui arch dam which has a height of 122.5m and a crest length of 510 m. The dam body was idealized by seventy-seven 16-node isoparametric shell elements shown in Fig.1. For the purpose of comparison, a conventional model

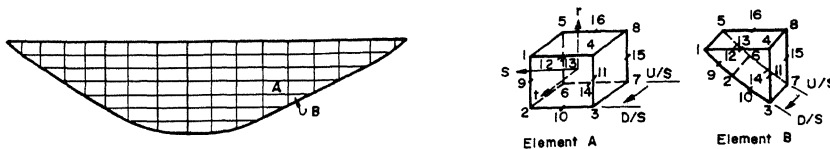


Fig. 1 Finite-Element Model of Feitsui Arch Dam

called Vogt's Constant Method was also adopted, in which the foundation effects were represented by three-component discrete springs connected to the nodes at the interface. The stiffness of each spring was obtained from Vogt's Constants. The results indicate that the corresponding mode shapes and frequencies are quite comparable between the two methods; however, the stresses obtained from the Strip Compliance Method are lower than those obtained from Vogt's Constant Method.

STRIP COMPLIANCE METHOD

Basic Equations Fig.2 shows an infinite rigid massless strip of width $2h$ resting on the surface of an elastic half-space with shear modulus G and subjected to unit harmonic moment and forces of $e^{i\omega t}$, per unit length of strip, in r , n , t and l -direction respectively. The rotation and displacements of this strip are given as:

$$\begin{aligned} u_r &= (C_{rr}/h^2G) \cdot e^{i\omega t} & (1a); & & u_t &= (C_{tt}/G) \cdot e^{i\omega t} & (1c) \\ u_n &= (C_{nn}/G) \cdot e^{i\omega t} & (1b); & & u_l &= (C_{ll}/G) \cdot e^{i\omega t} & (1d) \end{aligned}$$

where, $c_{rr}=R_r-iI_r$, $c_{nn}=R_n-iI_n$, $c_{tt}=R_t-iI_t$, $c_{ll}=R_l-iI_l$ are the compliance obtained respectively from Fig.3 (Ref.1); the coupling effects of c_{rt} and c_{tr} are neglected; V_s is the shear wave velocity of the foundation.

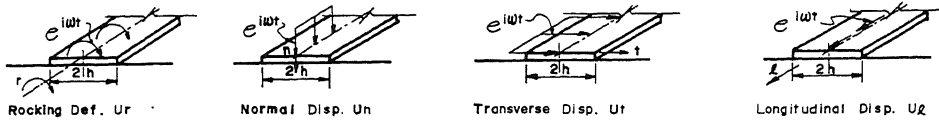


Fig. 2 Infinite Rigid Massless Strip of Width $2h$ Resting on Elastic Half-Space

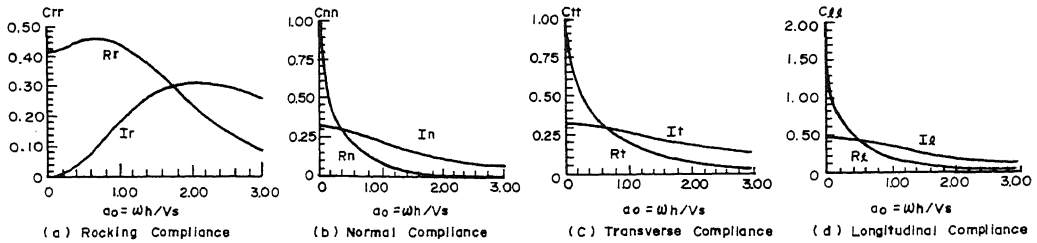


Fig. 3 Compliance of Infinite Rigid Massless Strip of Width $2h$

Foundation Dynamic Stiffness and Damping Fig.4 shows the developed area of the foundation's interface with the dam's finite element model. The foundation effects are represented by spring dash-pot sets, as shown in Fig.5, along the interface on each line connected between U/S and D/S nodes. The stiffness of springs k_r , k_n , k_t , k_l and damping of dash-pots c_r , c_n , c_t , c_l per unit length of interface are obtained from the compliance functions given in Fig. 3 by setting $2h=T$ (dam thickness).

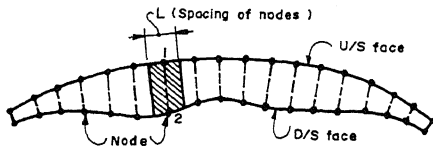


Fig. 4 Dam-Foundation Interface

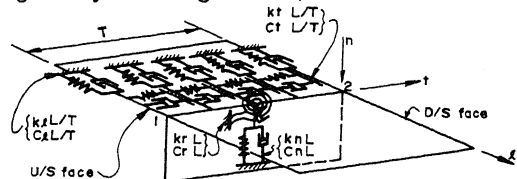


Fig. 5 Discrete Spring & Dash-Pot Sets

If the model shown in Fig.5 is subjected to a unit harmonic moment of $e^{i\omega t}$, per unit length, in r -direction, its equation of motion is expressed by:

$$c_r \dot{u}_r + k_r u_r = e^{i\omega t} \quad (2)$$

The rotation of this model in r -direction is given as:

$$u_r = (k_r + i\omega c_r)^{-1} \cdot e^{i\omega t} \quad (3)$$

Comparing Eq.(3) with Eq.(1a) and substituting $R_r - iI_r$ for C_{rr} gives the dynamic stiffness and damping of spring and dash-pot in r-direction as:

$$k_r = GT^2 R_r / [4(R_r^2 + I_r^2)] \quad (4a); \quad c_r = GT^2 I_r / [4\omega(R_r^2 + I_r^2)] \quad (4b)$$

Likewise, those in n, t and l-direction are given as:

$$k_n = GR_n / (R_n^2 + I_n^2) \quad (4c); \quad c_n = GI_n / [\omega(R_n^2 + I_n^2)] \quad (4d)$$

$$k_t = GR_t / (R_t^2 + I_t^2) \quad (4e); \quad c_t = GI_t / [\omega(R_t^2 + I_t^2)] \quad (4f)$$

$$k_l = GR_l / (R_l^2 + I_l^2) \quad (4g); \quad c_l = GI_l / [\omega(R_l^2 + I_l^2)] \quad (4h)$$

The dynamic stiffness and damping of spring dash-pot set shown in Eqs.(4) should be transformed to be consistent with nodal degrees of freedom along n,t and l-direction at nodes 1 and 2. Based on the Virtual Work Principle (Ref.2), each element of this consistent stiffness matrix and damping matrix can be derived from

$$K_{ij}^e = \int_0^T k(t) \cdot \Psi_i(t) \cdot \Psi_j(t) dt \quad (5); \quad C_{ij}^e = \int_0^T c(t) \cdot \Psi_i(t) \cdot \Psi_j(t) dt \quad (6)$$

where, $k(t)$ is $k_r L \delta(t-T/2)$, $k_n L \delta(t-T/2)$, $k_t L/T$, $k_l L/T$ respectively; $c(t)$ is $c_r L \delta(t-T/2)$, $c_n L \delta(t-T/2)$, $c_t L/T$, $c_l L/T$ respectively; shape functions, $\Psi_1(t)=1-t/T$, $\Psi_2(t)=t/T$ are for springs and dash-pots along t and l directions; $\Psi_1(t)=1/T$, $\Psi_2(t)=-1/T$ are for those along r direction; $\Psi_1(t)=\Psi_2(t)=1/2$ is for those along n direction. Operating Eqs.(5) and (6) obtains the consistent stiffness and damping matrices as follows:

$$\underline{K}_n^e = \begin{bmatrix} \frac{1}{4}k_n L + \frac{1}{T^2}k_r L & \frac{1}{4}k_n L - \frac{1}{T^2}k_r L \\ \frac{1}{4}k_n L - \frac{1}{T^2}k_r L & \frac{1}{4}k_n L + \frac{1}{T^2}k_r L \end{bmatrix} = \frac{LG_n}{4} \begin{bmatrix} \frac{R_n}{R_n^2 + I_n^2} + \frac{R_r}{R_r^2 + I_r^2} & \frac{R_n}{R_n^2 + I_n^2} - \frac{R_r}{R_r^2 + I_r^2} \\ \frac{R_n}{R_n^2 + I_n^2} - \frac{R_r}{R_r^2 + I_r^2} & \frac{R_n}{R_n^2 + I_n^2} + \frac{R_r}{R_r^2 + I_r^2} \end{bmatrix} \quad (7a)$$

$$\underline{K}_t^e = \begin{bmatrix} k_t L/3 & k_t L/6 \\ k_t L/6 & k_t L/3 \end{bmatrix} = (LG_i/6) \begin{bmatrix} 2R_t/(R_t^2 + I_t^2) & R_t/(R_t^2 + I_t^2) \\ R_t/(R_t^2 + I_t^2) & 2R_t/(R_t^2 + I_t^2) \end{bmatrix} \quad (7b)$$

$$\underline{K}_l^e = \begin{bmatrix} k_l L/3 & k_l L/6 \\ k_l L/6 & k_l L/3 \end{bmatrix} = (LG_i/6) \begin{bmatrix} 2R_l/(R_l^2 + I_l^2) & R_l/(R_l^2 + I_l^2) \\ R_l/(R_l^2 + I_l^2) & 2R_l/(R_l^2 + I_l^2) \end{bmatrix} \quad (7c)$$

$$\underline{C}_n^e = \begin{bmatrix} \frac{1}{4}c_n L + \frac{1}{T^2}c_r L & \frac{1}{4}c_n L - \frac{1}{T^2}c_r L \\ \frac{1}{4}c_n L - \frac{1}{T^2}c_r L & \frac{1}{4}c_n L + \frac{1}{T^2}c_r L \end{bmatrix} = \frac{LG_n}{4\omega} \begin{bmatrix} \frac{I_n}{R_n^2 + I_n^2} + \frac{I_r}{R_r^2 + I_r^2} & \frac{I_n}{R_n^2 + I_n^2} - \frac{I_r}{R_r^2 + I_r^2} \\ \frac{I_n}{R_n^2 + I_n^2} - \frac{I_r}{R_r^2 + I_r^2} & \frac{I_n}{R_n^2 + I_n^2} + \frac{I_r}{R_r^2 + I_r^2} \end{bmatrix} \quad (7d)$$

$$\underline{C}_t^e = \begin{bmatrix} c_t L/3 & c_t L/6 \\ c_t L/6 & c_t L/3 \end{bmatrix} = (LG_i/6\omega) \begin{bmatrix} 2I_t/(R_t^2 + I_t^2) & I_t/(R_t^2 + I_t^2) \\ I_t/(R_t^2 + I_t^2) & 2I_t/(R_t^2 + I_t^2) \end{bmatrix} \quad (7e)$$

$$\underline{C}_l^e = \begin{bmatrix} c_l L/3 & c_l L/6 \\ c_l L/6 & c_l L/3 \end{bmatrix} = (LG_i/6\omega) \begin{bmatrix} 2I_l/(R_l^2 + I_l^2) & I_l/(R_l^2 + I_l^2) \\ I_l/(R_l^2 + I_l^2) & 2I_l/(R_l^2 + I_l^2) \end{bmatrix} \quad (7f)$$

where, G_n and G_i are the shear moduli in the directions normal to and parallel to the foundation surface.

Some Approaches During Dynamic Stress Analysis The mode superposition method was applied in the time-history analysis. Since the stiffness and damping used in the computer program SAPIV should be frequency-independent, the frequency-dependent compliance and ω implied in the foundation stiffness and damping as shown in Eqs.(7) were approximately evaluated by taking the average values of the first few modes. To calculate the mode shapes and frequencies, the foundation stiffness should be included in the whole structure stiffness matrix. If ϕ is the matrix of mass-orthonormalized mode shapes, it is usually assumed that the damping matrix \underline{C}^s of structure only will diagonalize when operated on as given by:

$$\underline{\Delta}^s = \underline{\phi}^T \underline{C}^s \underline{\phi} = \begin{bmatrix} 2\omega_1 \xi_1 s_1 & & & 0 \\ & 2\omega_2 \xi_2 s_2 & & \\ & & \dots & \\ 0 & & & 2\omega_n \xi_n s_n \end{bmatrix} \quad (8)$$

where, numerical values of structure damping ratio $\xi_i s_i$ are usually assumed.

In order to include the foundation damping ratio ξ_{fi} into Eq.(8) for further

dynamic response and stress analysis, the damping ratio for each model in Eq.(8) should be corrected by the following procedures. First, using the foundation damping given in Eqs.(7d) to (7f) forms a damping matrix \underline{C}^f for the entire dam foundation system, and operates on \underline{C}^f as follows:

$$\Delta^f = \phi^T \underline{C}^f \phi \quad (9)$$

Ignoring the off diagonal terms of Δ^f and setting the diagonal terms equal to $2\omega_i \xi_{fi}$ ($i=1,2,\dots,n$) gives

$$\xi_{fi} = \Delta^f_{ii} / (2\omega_i) \quad i = 1, 2, \dots, n \quad (10)$$

where, $\Delta^f_{ii} = \phi_i^T \underline{C}^f \phi_i$

Then, the damping ratios ξ_{si} in Eq.(8) are to be replaced by damping ratios ξ_i as in Eq.(11) to include the effect of foundation radiation damping in the analysis.

$$\xi_i = \xi_{si} + \xi_{fi} \quad i = 1, 2, \dots, n \quad (11)$$

VOGT'S CONSTANT METHOD

Basic Equations The average rotation and deformations of a loaded rectangular area of the foundation surface due to unit moment, force and shear per unit length are given by Dr. Fredrick Vogt's equations (Ref. 3) as:

$$a' = k_1 / (E_n T^2); \quad \beta' = k_2 / E_n; \quad \gamma' = k_3 / E_i; \quad \delta' = (b/2a) \cdot (k_3 / E_i) \quad (12)$$

where, a' and β' are the rotation and deformation in the plane normal to the foundation surface; γ' and δ' are the deformation along transverse and longitudinal directions in the plane of the foundation surface respectively; E_n and E_i are the foundation effective deformation moduli normal to and parallel to the foundation surface; k_1 , k_2 and k_3 are Vogt's Constants (Ref.3).

Foundation Static Stiffness This method represents the foundation effects only by the spring sets, as shown in Fig. 5, excluding the dash-pot sets there. The stiffness of each spring per unit length along the interface is obtained just by inverting of the values of Eqs.(12). Thus,

$$k_r = E_n T^2 / k_1; \quad k_n = E_n / k_2; \quad k_t = E_i / k_3; \quad k_l = (2a/b) \cdot (E_i / k_3) \quad (13)$$

In applying Eq.(5), the spring stiffness of Eqs.(13) should be transformed into the stiffness as given in Eqs.(14), which are consistent with nodal degrees of freedom along n, t and l-direction respectively at nodes 1 and 2.

$$\underline{k}_n^e = L \begin{bmatrix} k_n/4+k_r/T^2 & k_n/4-k_r/T^2 \\ k_n/4-k_r/T^2 & k_n/4+k_r/T^2 \end{bmatrix} = LE_n \begin{bmatrix} 1/(4k_2)+1/k_1 & 1/(4k_2)-1/k_1 \\ 1/(4k_2)-1/k_1 & 1/(4k_2)+1/k_1 \end{bmatrix} \quad (14a)$$

$$\underline{k}_t^e = L \begin{bmatrix} k_t/3 & k_t/6 \\ k_t/6 & k_t/3 \end{bmatrix} = LE_i \begin{bmatrix} 1/(3k_3) & 1/(6k_3) \\ 1/(6k_3) & 1/(3k_3) \end{bmatrix} \quad (14b)$$

$$\underline{k}_l^e = L \begin{bmatrix} k_l/3 & k_l/6 \\ k_l/6 & k_l/3 \end{bmatrix} = (2aLE_i/b) \begin{bmatrix} 1/(3k_3) & 1/(6k_3) \\ 1/(6k_3) & 1/(3k_3) \end{bmatrix} \quad (14c)$$

In the dynamic analysis, each foundation stiffness as shown in Eqs.(14) was included in the structure stiffness matrix by the direct added method. The foundation radiation damping effect was neglected in this method.

EXAMPLE AND RESULTS

Example of Finding Foundation Compliance, Stiffness and Damping Ratio Basic data: f_1 (1st mode freq.)=1.784Hz; f_5 (5th mode freq.)=3.514Hz; $V_s=1500$ m/sec; $T=25$ m; $G_n = E_n/3$; $G_i = E_i/3$; $a_0 = \omega \cdot h / V_s = \pi f T / V_s$. From Fig. 3, the foundation compliance corresponding to the first mode and fifth mode were obtained respectively and were averaged as shown in Table 1.

Table 1 Foundation Compliance

	1st mode ($a_0=.093$)	5th mode ($a_0=.184$)	Average
R_r	0.41	0.42	0.42
I_r	0.00	0.00	0.00
R_n	0.62	0.46	0.54
I_n	0.33	0.33	0.33
R_t	0.76	0.60	0.68
I_t	0.33	0.33	0.33
R_l	0.98	0.78	0.88
I_l	0.49	0.49	0.49

Table 2 Foundation Stiffness Obtained from the Two Methods

	k_r	k_n	k_t	k_l
Vogt's Const.M.	$0.19E_n T^2$	$0.48E_n$	$0.39E_i$	$0.40E_i$
Strip Compli.M.	$0.20E_n T^2$	$0.45E_n$	$0.40E_i$	$0.29E_i$

Substituting the average compliance into Eqs.(4a), (4c), (4e) and (4g) gives the foundation dynamic stiffness as shown in Table 2. The foundation stiffness obtained by Vogt's Constant Method, using Eq.(13), is also shown in Table 2 for comparison. By using Eqs.(4b), (4d), (4f), (4h) the foundation damping matrices are calculated, and from Eq.(9) and Eq.(10) are obtained the foundation radiation damping ratios for the first 30 modes as shown in Fig. 6.

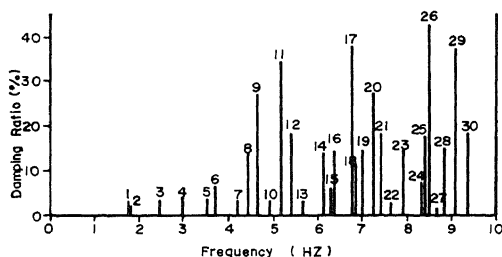


Fig. 6 Foundation Radiation Damping Ratio

Table 3 Model Frequencies

Mode	Vogt's Const. M.	Strip Compl. M.
1	1.784	1.785
2	1.806	1.809
3	2.457	2.471
4	2.937	2.962
5	3.514	3.542
6	3.739	3.738
7	4.167	4.198
8	4.441	4.441
9	4.854	4.630
10	4.966	4.890

Results The first ten-mode frequencies and mode shapes of the dam crest obtained by the two methods are shown in Table 3 and Fig.7. Table 4 summarizes the tensile stresses of over 525 t/m^2 under the extreme loading condition for three components of time-history record with peak acceleration of 0.4g, 0.3g and 0.24g along upstream-downstream, cross-canyon and vertical directions respectively.

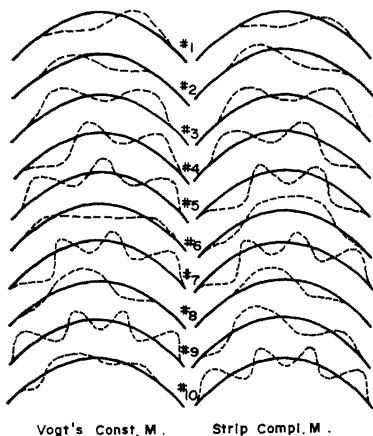


Fig. 7 Mode Shapes of Dam Crest

Table 4 Summary of Tensile Stresses of over 525 t/m^2

Method	Occur- ring time (sec.)	Distri- bution Area (elements)	Dura- tion (sec.)	Max. Tensile Stress (t/m^2)*
Vogt's Const. Meth.	3.33	1	0.02	560 C,D
	3.57	1	0.05	619 A,D
	4.24	2	0.08	697 A,U
	4.83	1	0.06	624 A,U
	5.42	3	0.11	641 C,U
	6.42	7	0.14	778 C,U
	6.60	2	0.09	692 A,D
Strip Compl. Meth.	7.20	1	0.06	580 C,U
	4.24	2	0.06	593 A,U
	5.42	1	0.04	558 C,U
	6.42	4	0.11	648 C,U
	6.60	1	0.02	544 A,D

*: C=Cant., A=Arch, D=D/S face, U=U/S face

DISCUSSIONS AND CONCLUSIONS

1. In the Strip Compliance Method and Vogt's Constant Method, the effects of geological conditions on the foundation were adequately reflected by the effective deformation moduli E_n and E_i , which varied according to the geological conditions along the foundation interface and were obtained separately by a series of analyses of two-dimensional finite element models of foundation at some representative locations along the interface (Ref.4). In these 2-D models, the major weak planes of 100% continuity existing in the foundation were included as joint elements, and those joints and fissures not of 100% continuity were not included but their effects were considered by using the joint-shear index (Ref.5) to modify the elastic moduli of rock mass elements obtained from the lab.

2. Table 3 and Fig.7 show that the frequencies and mode shapes obtained from the two methods are almost the same. This is because the foundation stiffness obtained from the two methods are quite close as shown in Table 2. A comparison of dam stresses indicates that the stresses obtained from the Strip Compliance Method are, in general, smaller than those obtained from Vogt's Constant Method. Table 4 shows that the maximum tensile stress is about 16.7% less, and the occurring times, distribution area and duration of the stresses of over 525 t/m² that occurred in the stress history are also less, smaller and shorter. These phenomena are attributable to the effects of the foundation radiation damping considered in the Strip Compliance Method.

3. Vogt's Constant Method has been applied in the Trial-Load Method (Ref.3) for dam stress analysis. After transformation as described in this paper, it can also be efficiently applied in the Finite-Element Method. For the dynamic stress analysis, the use of Vogt's Constant Method can get stresses on the conservative side.

4. Since the Strip Compliance Method can simply and properly represent the foundation effects with not only stiffness but also radiation damping, it is concluded that this method is quite adequate and efficient for the seismic response analysis of arch dams and other kinds of structures.

ACKNOWLEDGEMENTS

The author is grateful to Prof. Joseph Penzien for providing the concept, basic data and valuable instructions, and to Dr. Hsiang-Chuan Tsai for developing the computer programs and performing the analyses.

REFERENCES

1. Tzong, T.J., Gupta, S., Penzien, J., "Two-Dimensional Hybrid Modelling of Soil-Structure Interaction," University of California, Berkeley, Earthquake Engineering Research Center, Report No. UCB/EERC-81/11, (1981).
2. Clough, R.W., Penzien, J., "Dynamics of Structures," McGraw Hill, (1975).
3. "Design of Arch Dams," United States Department of the Interior Bureau of Reclamation, Denver, Colorado, (1977).
4. Feitsui Reservoir Project, "Determination of the Foundation Effective Deformation Modulus for Dam Stress Analysis," BDR-24, Sinotech Engineering Consultants, Inc., Taipei, Republic of China (1980).
5. Feitsui Reservoir Project, "Determination of the Deformation Modulus of Foundation Rock Masses," BDR-22, Sinotech Engineering Consultants, Inc., Taipei, Republic of China (1980).